A Markov Chain Monte Carlo technique for Galactic cosmic-ray physics

A. Putze*, **L. Derome***, **D. Maurin**†

Laboratoire de Physique Subatomique et de Cosmologie LPSC, Grenoble, France

†*Laboratoire de Physique Nucléaire et des Hautes Energies LPNHE, Paris, France*

***Abstract*. We implemented a Markov Chain Monte Carlo technique to estimate the probability density functions of the cosmic-ray transport and source parameters. The results of the Leaky-Box and the 1D diffusion model are presented. In the Leaky-Box model, our best fit to B/C data favours both a low energy cut-off and reacceleration. For the diffusion model, we included constraints from the radioactive nuclei to break the degeneracy between the diffusion coefficient normalisation K_0 and the halo size L of the Galaxy.**

***Keywords*: Cosmic rays - MCMC**

I. INTRODUCTION

One issue of cosmic-ray (CR) physics is the determination of the transport parameters in the Galaxy. Such a determination is based on the analysis of the secondary-to-primary ratio (e.g. B/C, sub-Fe/Fe). The method to extract these parameters in the past has been mostly based on a manual or semi-automated—hence partial—coverage of the parameter space (e.g., [1], [2], [3]). More complete scans have been performed ([4], [5], [6]), but in an inefficient manner. The addition of a single new free parameters in the standard grid-scan approach remains prohibitive in terms of computer time.

Therefore it is necessary to use an efficient and sound numerical tool to i) cover efficiently the parameter space and ii) enable the enlargement of the parameter space at a minimal computing time cost. The Markov Chain Monte Carlo (MCMC) algorithm, widely used for cosmological parameter estimates (see e.g. [7], [8] and references therein), meets these demands. The MCMC algorithm provides the probability density function (PDF) of the model parameters, based on selected experimental data. A detailed description of the approach used is given in [9].

The model parameter values presented here correspond to the most probable values, i.e., the peak value of the marginalised parameter PDFs, whereas the χ^2 values represent the best-fit model for which the parameter values are not given.

II. RESULTS FOR THE LEAKY-BOX MODEL (LBM)

We use the LBM with minimal reacceleration [10], where the grammage $\lambda_{\rm esc}(R)$ is parametrised as

$$\lambda_{\rm esc}(R) = \begin{cases} \lambda_0 \beta R_0^{-\delta} & \text{when } R < R_0, \\ \lambda_0 \beta R^{-\delta} & \text{otherwise.} \end{cases} \quad (1)$$

TABLE I

MOST PROBABLE VALUES FOR DIFFERENT MODELS (B/C DATA ONLY). THE UNCERTAINTIES CORRESPOND TO 68% CL OF THE MARGINALISED PDF. THE DIFFERENT DATA SETS ARE A=HEAO-3 (14 DATA POINTS), C=HEAO-3+ ACE+VOYAGER 1 & 2+IMP7-8 (22 DATA POINTS), D= HEAO-3+ALL LOW-ENERGY DATA (30 DATA POINTS).

Model Data	λ_0 $({\rm g\,cm^{-2}})$	R_0 (GV)	δ	$\mathcal{V}_a$ $({\rm km\,s^{-1}kpc^{-1}})$	$\chi^2_{\rm min}$/dof
I-A	54^{+2}_{-2}	$4.2^{+0.3}_{-0.9}$	$0.70^{+0.01}_{-0.01}$	...	3.35
II-A	26^{+2}_{-2}	...	$0.52^{+0.02}_{-0.02}$	88^{+6}_{-11}	1.43
III-A	30^{+5}_{-4}	$2.8^{+0.6}_{-0.8}$	$0.58^{+0.01}_{-0.06}$	75^{+10}_{-13}	1.30
III-C	27^{+2}_{-2}	$2.6^{+0.4}_{-0.7}$	$0.53^{+0.02}_{-0.03}$	86^{+9}_{-5}	1.06
III-D	26^{+2}_{-2}	$3.0^{+0.4}_{-0.5}$	$0.52^{+0.02}_{-0.02}$	95^{+7}_{-6}	4.15

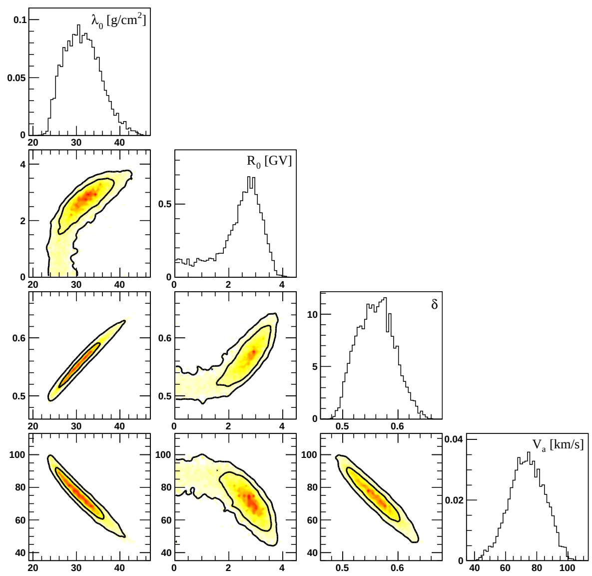

Fig. 1. PDFs for the LBM (Model III-A, see Table I). The diagonal plots show the 1D marginalised PDF of the indicated parameters. Off-diagonal plots show the 2D marginalised PDF for the parameters in the same column and same line respectively. The colour code corresponds to the regions of increasing probability (from paler to darker shade). The two contours (smoothed) delimit regions containing respectively 68% and 95% (inner and outer contour) of the PDF.

Based on HEAO-3 B/C data, the values obtained for the model without reacceleration (Model I, see Table I) are similar to those derived by [11]. In agreement with previous studies, we confirm that a model with a rigidity cutoff performs more successfully than one without and that reacceleration is preferred over no reacceleration (compare $\chi^2_{\rm min}$ values of Models I to III in Table I).

The PDFs of the parameters and correlations for the LB model parameters are given in Fig. 1. As found in [4], the best-fit models demand both a rigidity cutoff (wind) and reacceleration, but do not allow us to reconcile the diffusion slope with a Kolmogorov spectrum for turbulence ($\delta = 1/3$). Note however, that a model without rigidity cutoff is not excluded.

Various subsets of B/C data (A, C, and D, see Table I) were used to investigate whether old data (e.g. data from ISEE-3 and Ulysses) are useful or just add confusion to the PDF determination. The ISEE-3 and Ulysses data points are found inconsistent with other low-energy data (compare Model III-D with III-C in Table I); the $\chi^2_{\rm min}$ is worsened. We also find that using different B/C data sets leaves mostly unchanged the propagation parameters, only affecting the assessment of the goodness of a model.

Taking advantage of the knowledge of the χ^2 distribution, we can extract a list of configurations (parameter sets), based on CLs of the χ^2 PDF. These parameter sets are used to draw confidence envelopes on the fluxes. Figure 2 demonstrates that current data are already able to constrain strongly the B/C flux, even at high energy.

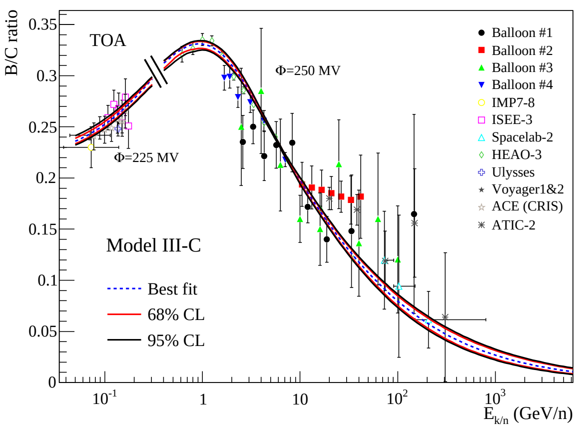

Fig. 2. Confidence regions of the B/C ratio for the LBM. The blue-dashed line is the best-fit solution, red-solid line is 68% CL and black-solid line 95% CL. Modulation parameter: $\Phi =$ 225 MV below 0.4 GeV/n (for ACE+Voyager 1 & 2+IMP7-8 data) and $\Phi = 250$ MV above (for HEAO-3 data).

In all previous studies, the source parameters were investigated after the propagation parameters had been determined from the B/C ratio (or other secondary-to-primary ratio). We propose a more general approach where we fit simultaneously both the source and the transport parameters. We find correlations between the propagation and source parameters, biasing the estimates of these parameters. The best-fit model slope for the source abundances is $\alpha \approx 2.17$ using HEAO-3 oxygen data, compatible with the value $\alpha \approx 2.14$ for TRACER oxygen data (see Fig. 3).

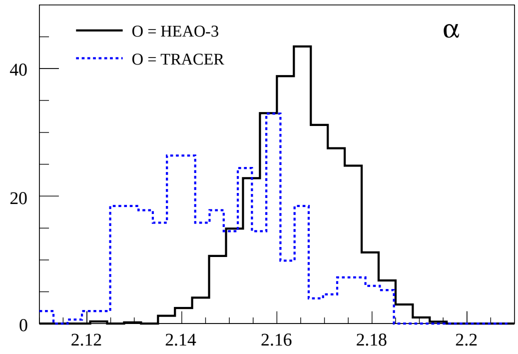

Fig. 3. PDF for the source slope α. Oxygen data for the fit are HEAO-3 (solid-black line) or TRACER (blue-dashed line).

III. Results for the 1D Diffusion Model (DM)

We also consider the 1D thin disc Diffusion Model [3] with constant Galactic wind V_c and minimal reacceleration. The diffusion coefficient is given by

$$K(R) = K_0 \beta R^{\delta}. \tag{2}$$

This model is shown in Fig. 4. The free parameters of this model are the halo size L of the Galaxy, the constant Galactic wind V_c, the normalisation K_0 and the slope δ of the diffusion coefficient $K(E)$, and finally the Alfvén velocity V_a related to the reacceleration.

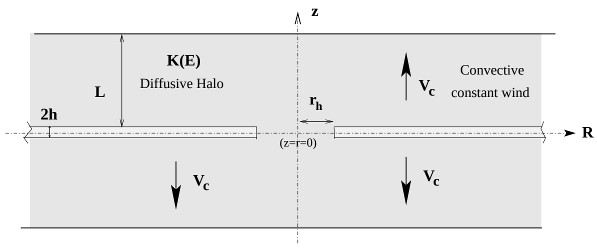

Fig. 4. Sketch of the 1D model: sources and interactions (including energy losses and gains) are restricted to the thin-disc $\propto 2h\delta(r)$. Diffusion K and convection V_c transport nuclei in the disc (half-height h) and in the halo (half-height L). For simplicity, the local bubble is featured as a hole of radius r_h in the disc and is assumed to affect only the radioactive species [see Eq. (5)].

The standard DM can be modified in order to take into account the under-dense local interstellar medium (LISM) [12]. It is modelled as a hole in the Galactic disc [13].

A. Standard Model: stable nuclei

We start with the standard DM ($r_h = 0$), since the local bubble affects only the radioactive nuclei discussed in the next section. There is a well-known degeneracy between the parameters K_0 and L when stable species are considered: all models with the same ratio K_0/L lead to the same grammage,

$$\lambda_{\rm esc} = n\bar{m}vhL/K(E), \tag{3}$$

hence to the same secondary-to-primary ratio.

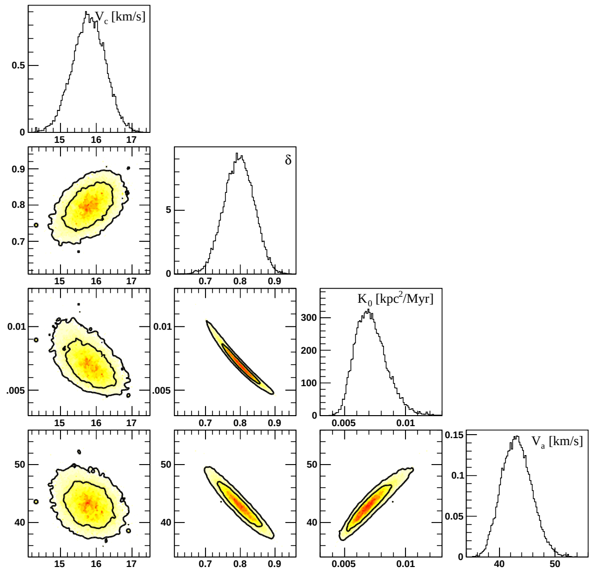

Fig. 5. PDFs for the DM for parameters $\{V_c,\ \delta,\ K_0,\ V_a\}$ with L fixed to 4 kpc.

Here we used B/C data only and we fixed $L = 4\,\mathrm{kpc}$. The PDFs for Model III-C are shown in Fig. 5 and the parameter values are shown in Table II.

TABLE II
MOST PROBABLE VALUES OF THE FREE PARAMETERS FOR THE STANDARD DIFFUSION MODEL, USING B/C DATA

Model Data	$K_0 \times 10^2$ ($\mathrm{kpc^2 Myr^{-1}}$)	δ	V_c ($\mathrm{km\,s^{-1}}$)	V_a ($\mathrm{km\,s^{-1}}$)	$\chi^2_{\rm min}$/dof
I-C	$0.42^{+0.04}_{-0.03}$	$0.97^{+0.02}_{-0.02}$	$9.7^{+0.2}_{-0.3}$	$\cdots$	16.64
II-C	$6.2^{+0.2}_{-0.2}$	$0.349^{+0.005}_{-0.008}$	$\cdots$	75^{+2}_{-2}	3.63
III-C	$0.7^{+0.2}_{-0.1}$	$0.79^{+0.05}_{-0.04}$	$15.8^{+0.4}_{-0.5}$	43^{+3}_{-2}	1.52

As for the LBM, a model with a Galactic wind performs more successfully than one without, and reacceleration is preferred over no reacceleration (compare $\chi^2_{\rm min}$ of Models I to III in Table II). We confirm the results found in [4], [5]: large δ are obtained. Only Model II (with reacceleration but without wind) is close to the Kolmogorov spectrum of 1/3, but this model is not favoured by the data.

The value for δ found in the DM is larger than that found for the LBM. For the chosen energy dependence of $K(E)$, the equivalent LB grammage for the DM [Eq. (2) and Eq. (3)] differs from a β factor compared to the standard LB grammage Eq. (1):

$$\lambda_{\rm esc}^{\rm DM} = \lambda_0 R^{-\delta} \quad \text{vs} \quad \lambda_{\rm esc}^{\rm LBM} = \lambda_0 \beta R^{-\delta}\ . \qquad (4)$$

We explicitly checked that the same δ was recovered (from the B/C fit) between the LBM and the DM when using $\lambda_{\rm esc}^{\rm DM}$ in the LBM.

B. Standard Model: radioactive nuclei

The degeneracy between K_0 and L is lifted when radioactive secondary nuclei are considered. At low energy the distance travelled by a radioactive nucleus is $l_{\rm rad} = \sqrt{K\gamma\tau_0}$. Using $K \approx 10^{28}\,\mathrm{cm^2 s^{-1}}$ and $\tau_0 \approx 1$ Myr, the diffusion length is $l_{\rm rad} \approx 200$ pc. This nucleus doesn't reach the border of the Galaxy and is hence only sensitive to the diffusion coefficient K_0 [13].

We now let L as a free parameter and use ^{10}Be/^{9}Be (additionally to the B/C data) to constrain it. This radioactive ratio has no impact on the transport parameter values. They remain as given in Table II and as represented in Fig. 5. The PDF of L and its correlation with the transport parameters are shown in Fig. 6. We find $L = 19^{+2}_{-5}\,\mathrm{kpc}$, i.e., values significantly larger than those quoted in the literature.

C. Modified Model: radioactive nuclei with $r_h \neq 0$

In the last step the radius of the under-density in the LISM is added as a free parameter. The net effect of the local bubble is that the ratio of the flux calculated for a cavity/hole r_h to that of the flux with no hole ($r_h = 0$) is

$$\frac{N_{r_h}}{N_{(r_h=0)}} = \exp\left(\frac{-r_h}{\sqrt{K\gamma\tau_0}}\right) = \exp\left(\frac{-r_h}{l_{\rm rad}}\right)\ . \qquad (5)$$

The resulting PDFs for L and r_h are shown in Fig. 7. The most likely values and uncertainties at 68% CL of the two parameters are $L = 2^{+7}_{-1}\,\mathrm{kpc}$ and $r_h = 73^{+2}_{-2}\,\mathrm{pc}$. The local bubble parameter is correlated to the halo size of the Galaxy: the halo size L is lowered to the range 1 – 10 kpc when $r_h \neq 0$. The reduced χ^2 value of the best fit for this model is 1.31, which is better than 1.47 for the model with no hole. This confirms the findings of [13]: The standard model $r_h = 0$ is disfavoured. The bubble radius is consistent with the estimations from direct measurements.

The corresponding 98% CL envelopes on the ^{10}Be/^{9}Be ratio are shown (along with the best fit) in Fig. 8. The best fit for the hole model gives a higher ratio, closer to the ISOMAX data points. Other and better data on the radioactive nuclei are required in order to better constrained the L and r_h parameters. A more detailed study of the DM will be presented in Putze et al. (in preparation).

IV. CONCLUSION

We have implemented a Markov Chain Monte Carlo to extract the posterior distribution functions of the propagation parameters. Taking advantage of its sound statistical properties, confidence intervals for the propagation parameters can be given, as well as confidence contours for fluxes and other quantities derived from the propagation parameters. The MCMC was also used to compare the impact of choosing different data sets and ascertain the merits of different hypotheses concerning the propagation models.

In the LBM, in agreement with previous studies, we confirm that a model with a rigidity cutoff performs more successfully than one without and that reacceleration is preferred over no reacceleration. The

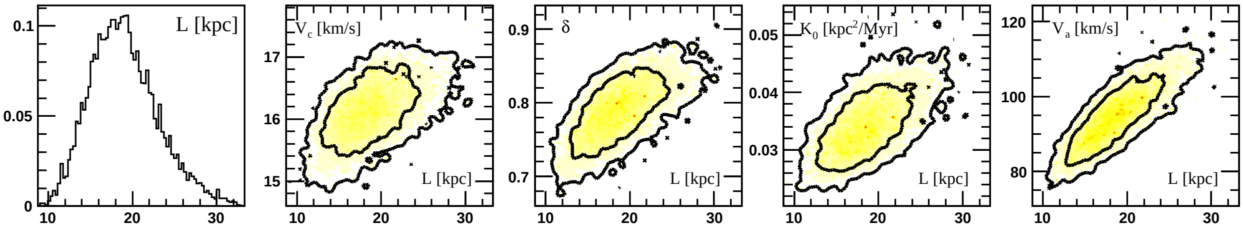

Fig. 6. PDF of the halo size L and its correlations with the transport parameters using B/C and ^{10}Be/^{9}Be data.

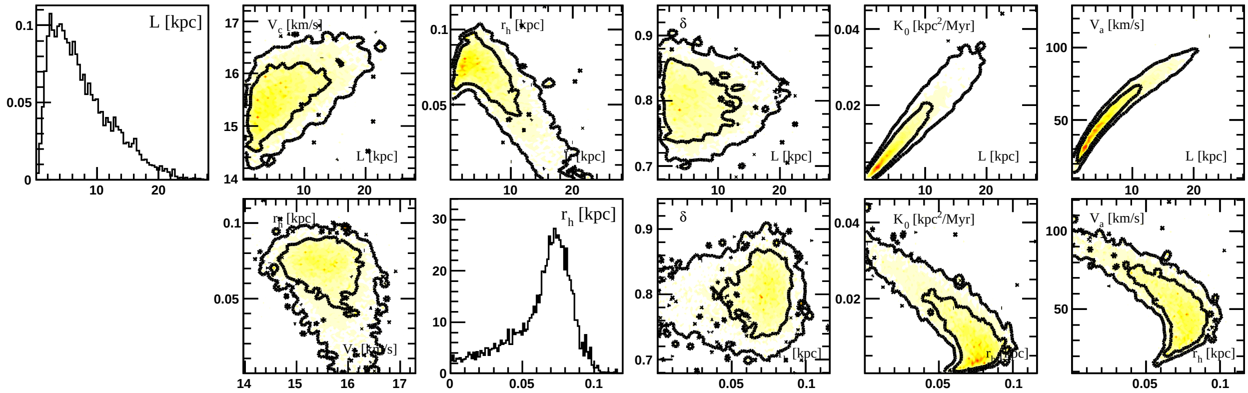

Fig. 7. Same data used as in Fig. 6, but for the modified model including the free parameter r_h. PDF of L (first row) and r_h (second row) with the correlations to the other parameters. Adding the hole increases the degeneracy between the parameters, nevertheless $r_h \neq 0$ is preferred.

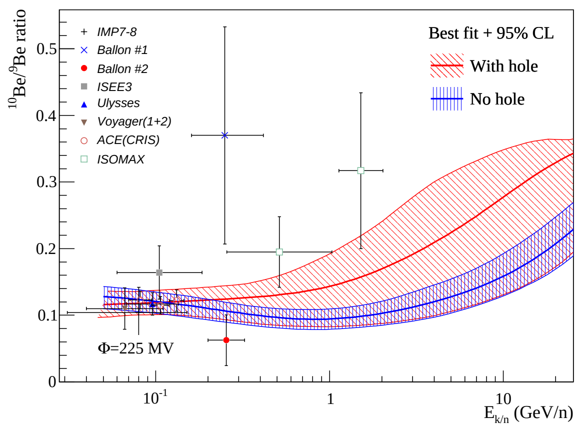

Fig. 8. 95% confidence regions (shaded areas) and best bit (thick-solid lines) of the ^{10}Be/^{9}Be ratio for the standard and modified DM.

best-fit models demand both a rigidity cutoff (wind) and reacceleration, but do not allow us to reconcile the diffusion slope with a Kolmogorov spectrum for turbulence. We additionally allowed the abundance and slope of the source spectra to be free parameters. This illustrated a correlation between the propagation and source parameters, potentially biasing the estimates of these parameters. The best-fit model slope for the source abundances was $\alpha \approx 2.17$ using HEAO-3 data, compatible with the value $\alpha \approx 2.14$ for TRACER data. The reader is referred to [9] for a complete report on the LBM analysis and results.

The same analysis was performed for the one-dimensional DM. The preliminary results confirm that a Kolmogorov spectrum is disfavoured by existing data. The best-fit model includes both convection and reacceleration for the transport of CR. We use the ^{10}Be/^{9}Be ratio to lift the degeneracy between K_0 and L. For the first time, we show the PDF of the halo size L. The uncertainty on L remains large due to the limited energy range covered by the radioactive nuclear data. We note that, for the standard DM (no hole), the value found for L is larger than that claimed in other studies. We also present the PDF of the local bubble size parameter, r_h, pointing to a value ~ 70 pc. The presence of an underdensity in the LISM is favoured by CR data. The effect of including a bubble is a reduction of the Galactic halo size L to a range of $1 - 10$ kpc when $r_h \neq 0$.

REFERENCES

[1] W. R. Webber, M. A. Lee, and M. Gupta, *ApJ* **390**, 96 (1992)
[2] A. W. Strong and I. V. Moskalenko, *ApJ* **509**, 212 (1998)
[3] F. C. Jones *et al.*, *ApJ* **547**, 264 (2001)
[4] D. Maurin *et al.*, *ApJ* **555**, 585 (2001)
[5] D. Maurin *et al.*, *A&A* **394**, 1039 (2002)
[6] A. M. Lionetto *et al.*, *JCAP* **9**, 10 (2005)
[7] A. Lewis and S. Bridle, *PRD* **66**, 103511 (2002)
[8] J. Dunkley *et al.*, *MNRAS* **356**, 925 (2005)
[9] A. Putze *et al.*, *A&A* **497**, 991 (2009)
[10] E. S. Seo and V. S. Ptuskin, *ApJ* **431**, 705 (1994)
[11] W. R. Webber *et al.*, *ApJ* **508**, 940 (1998)
[12] R. Lallement *et al.*, *A&A* **411**, 447 (2003)
[13] F. Donato *et al.*, *A&A* **381**, 539 (2002)